





Article

Physical-Chemical Properties Modification of *Hermetia Illucens* Larvae Oil and Diesel Fuel for the Internal Combustion Engines Application

Talal Yusaf ^{1,2} , Mohd Kamal Kamarulzaman ^{3,*} , Abdullah Adam ⁴ , Sakinah Hisham ³ ,
Devarajan Ramasamy ⁴ , Kumaran Kadirgama ^{3,4}, Mahendran Samykano ⁵ and Sivaraos Subramaniam ⁶

¹ School of Engineering and Technology, Central Queensland University, Brisbane, QLD 4009, Australia

² Institute of Sustainable Energy, Universiti Tenaga Nasional, Kajang 43000, Selangor, Malaysia

³ Advanced Nano Coolant-Lubricant (ANCL) Lab, Automotive Engineering Centre, Universiti Malaysia Pahang, Pekan 26600, Pahang, Malaysia

⁴ Faculty of Mechanical and Automotive Engineering Technology, Universiti Malaysia Pahang, Pekan 26600, Pahang, Malaysia

⁵ Department of Mechanical Engineering, College of Engineering, Universiti Malaysia Pahang, Gambang 26300, Pahang, Malaysia

⁶ Faculty of Manufacturing Engineering, Universiti Teknikal Malaysia Melaka, Durian Tunggal 76100, Melaka, Malaysia

* Correspondence: kamalkz@hotmail.com or kamalkz@ump.edu.my



Citation: Yusaf, T.; Kamarulzaman, M.K.; Adam, A.; Hisham, S.; Ramasamy, D.; Kadirgama, K.; Samykano, M.; Subramaniam, S. Physical-Chemical Properties Modification of *Hermetia Illucens* Larvae Oil and Diesel Fuel for the Internal Combustion Engines Application. *Energies* **2022**, *15*, 8073. <https://doi.org/10.3390/en15218073>

Academic Editor: Theodoros Zannis

Received: 15 September 2022

Accepted: 21 October 2022

Published: 31 October 2022

Publisher's Note: MDPI stays neutral with regard to jurisdictional claims in published maps and institutional affiliations.



Copyright: © 2022 by the authors. Licensee MDPI, Basel, Switzerland. This article is an open access article distributed under the terms and conditions of the Creative Commons Attribution (CC BY) license (<https://creativecommons.org/licenses/by/4.0/>).

Abstract: The use of insects as a biofuel feedstock has received limited research, and little is known about the fuel characteristics of insect biofuel. Fuel properties characterization can guide researchers focused on renewable fuel for the internal combustion engine. Therefore, this investigation focused on the physical-chemical properties modification of *Hermetia illucens* larvae oil (HILO) and diesel fuel blends, which could highly become an alternative renewable fuel. Five test fuel blends of HILO and diesel fuel were prepared at 0%, 25%, 50%, 75%, and 100% on a volume basis. Fuel properties such as chemical composition, density, viscosity, heating value, cetane number, and flash point of the test fuel blends were analyzed and compared to the diesel fuel. The main physical-chemical properties of HILO-diesel fuel blends were determined following the ASTM standards. Based on the results, the density, viscosity, cetane number, and flash point of the diesel fuel-HILO fuel blends were increased by 11.28%, 740.30%, 16.92%, and 86.67%, respectively, with the addition of HILO, except for the heating value reduced by 13.66%.

Keywords: physical-chemical properties; renewable fuel; biofuel; *Hermetia illucens*

1. Introduction

Many countries face severe challenges to sustainable growth and industrialization due to the growing fuel prices and environmental deterioration [1,2]. One of the consequences of these challenges is the hunt for renewable energy sources that fulfill world requirements for engine emissions and performance [3]. To overcome these challenges, most approaches for managing diesel engine emissions have been divided into pre-combustion and post-combustion control methods [4]. One of the pre-combustion control methods for reducing diesel engine emissions involved using biofuels such as bioethanol and biodiesel. Biofuel is a potential alternative to existing diesel due to its low sulphur contents, relatively high cetane number, biodegradability, renewability, and portability [5,6]. Even though biofuel may be produced by the direct blending method, other methods for producing biofuel include catalytic cracking, thermal cracking, micro-emulsification, and transesterification of fats and oils [7,8].

Biodiesel may be made from both edible crops (peanut oil, sunflower oil, rapeseed oil, palm oil, and soybean oil) and non-edible crops (rubber oil, linseed oil, castor oil, neem oil,

karanja oil, stillingia oil, and jatropha oil) oils [9]. The crop's market value, the country's climatic conditions, and geographical location determine the selection of a suitable crop for biofuel production in every country [10,11]. For example, sunflower and rapeseed oils are used as feedstock for Europe's biofuel production [12]. In contrast, coconut oil and soybean oil are utilized as feedstock for biofuel production in the Philippines and the United States [13]. However, most biofuel research is currently focusing on producing biofuel from alternative feedstocks such as insect oil [14], seaweeds [15], microalgae [16], grease [17], and waste oils [18]. The main downside of edible and non-edible crops is that their use for biofuel production jeopardizes the world food and feed supply chain by imposing a demand on agricultural land [19]. Furthermore, biofuel production from grease, algae, and seaweeds is believed to be one of the most effective ways of recycling waste generated by various environmental remediation schemes [20,21].

The utilization of insects in biofuel production is connected with the fact that insects can accumulate metabolic reserves named fat bodies, which they utilize during non-feeding times of their life cycle [22,23]. The insects' fat bodies play an important function in their metabolic processes and are used as medication and food by animals and humans [24]. Manzano-Agugliaro, et al. [25] found that the fat content of most insect species ranged between 25% and 77% and proposed that the excess fat may be utilized to produce biofuel. Li, et al. [26] investigated the biofuel potential of black soldier fly (also known as *Hermetia illucens*) larvae reared on 1 kg of chicken dung for 10 days. They discovered that the biodiesel produced by the black soldier fly larvae biofuel had equivalent fuel qualities compared to rapeseed-oil-based biodiesel, including cetane number (53), flash point (123 °C), ester content (97.2%), viscosity (5.8 mm²s⁻¹), and density (885 kg/m³). According to Surendra, et al. [27], the black soldier fly oil's potential for producing high-quality biodiesel is attributed to its low content of polyunsaturated fatty acids (13% total fatty acids) and high content of medium chain saturated fatty acids (67% total fatty acids).

The larvae of the black soldier fly, *Hermetia illucens* L., which can colonize a variety of organic materials (including animal dung, food waste, and fermentation straw), can utilize the waste nutrition for growth in which high levels of protein and fat were generated [28]. It has four life phases (i.e., egg, larva, pupa, and adult) [29]. Due to their ability to survive on fat reserves since they were larvae, adult flies are neither a bothersome species nor a mechanical carrier of disease [30,31]. Mating occurs two days after emergence, and oviposition takes place two days following fertilization [32]. Depending on the temperature and the availability of food, larval growth takes two to four weeks [33]. It has been demonstrated that the lipids from the energy insect larvae, which are transformed from organic wastes such restaurant garbage, are a unique and easily obtainable feedstock for biodiesel [34]. According to reports, the larva typically comprise 35–40% lipids and 40–44% crude proteins [35]. In comparison to higher plants or microalgae, the energy insect has specific benefits such as fast growth rate, high biomass production, shorter growing period, and minimal land use. They may also be cultivated in poultry manure and restaurant garbage, which helps to lessen the problem of urban pollution. Moreover, Kamarulzaman, et al. [36] had investigated the possibility of using biofuel from *Hermetia illucens* larval oil as a potential alternative fuel in a single cylinder direct injection compression ignition engine. The results revealed a 3.28% decrease in cylinder pressure, an 8.21% loss in brake thermal efficiency, and an increase in brake specific fuel consumption. Additionally, there was a downward trend in NO_x and O₂ of roughly 19.62% and 1.84%, respectively. Despite this, there was a rise in CO, CO₂, HC, and exhaust gas temperature. The researchers came to the conclusion that *Hermetia illucens* larval oil has a great potential to be used in compression ignition engines in the future.

Despite the promising potential of biofuel from insect feedstock [37], almost no study on the fuel characteristics of biofuel from *Hermetia illucens* larval oil has been reported. Evaluation of the most important fuel properties can assist researchers who focus on finding suitable renewable fuel for the diesel engine. Therefore, this study aims to characterize the most important physical and chemical fuel properties of *Hermetia illucens* larvae oil (HILO)-

diesel fuel blends compared to the baseline fuel. Five different HILO-diesel fuel blends were prepared, and the fuel properties such as chemical composition, density, viscosity, heating value, cetane number, and flash point were determined and analyzed.

2. Materials and Methods

This segment describes the experimental setup for test fuel preparation and physical-chemical properties measurements. The experimental setup clarifies the apparatus used and explains the methodology for fuel properties measurement, comprising the chemical composition, CHNOS elements, density, viscosity, heating value, cetane number, and flash point. The schematic diagram of the research strategy framework is illustrated in Figure 1.

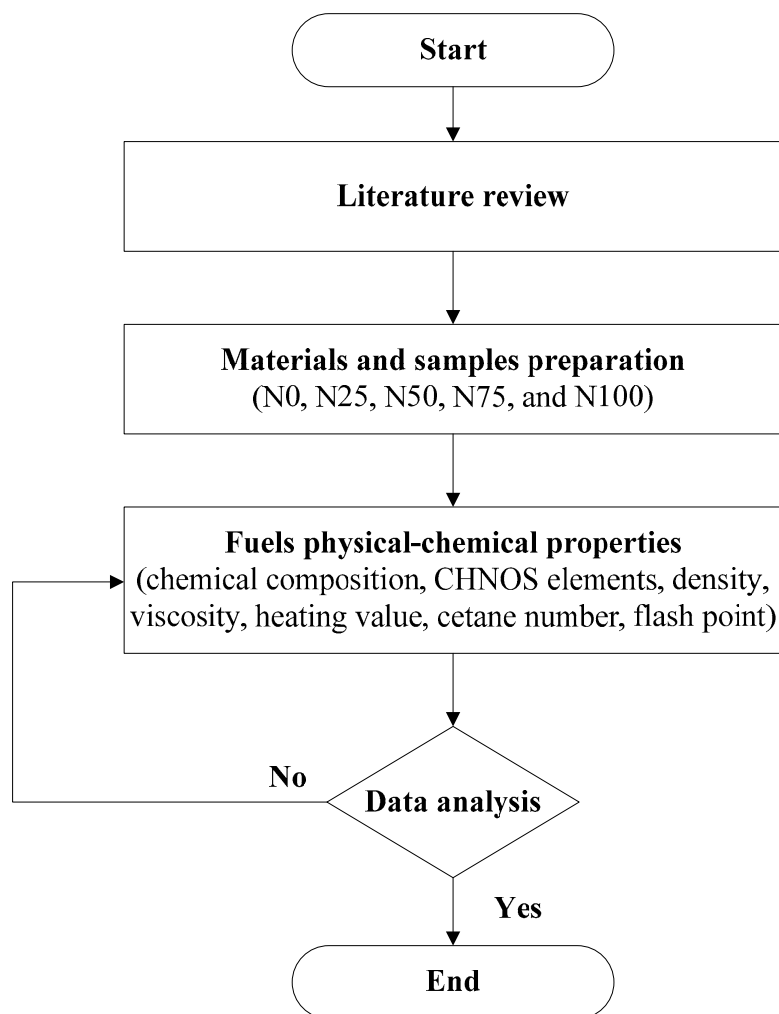


Figure 1. Schematic diagram of the research strategy framework.

2.1. Materials

The neat *Hermetia illucens* larvae oil used in this study was purchased from Entofood (Malaysia). Meanwhile, the baseline diesel fuel (DF) Euro 2M was obtained from a certified domestic fuel supplier, Rahar Jati Sdn. Bhd. In this study, five different fuel samples at different volume percentages were prepared using a mechanical mixing process through a direct blending method. The samples were labelled by N0 (100% DF, 0% HILO), N25 (75% DF, 25% HILO), N50 (50% DF, 50% HILO), N75 (25% DF, 75% HILO), and N100 (0% DF, 100% HILO) as shown in Figure 2 and summarized in Table 1. The required amount of HILO was initially transferred into a mixing container, followed by the diesel fuel portion. The mixture of diesel fuel and HILO were mixed thoroughly at room temperature using an IKA mechanical overhead stirrer RW20 digital for 15 min. To prevent the influence of

water vapor in the air, the fuel samples were heated during the preparation process to prevent water vapor from forming condensation. The mixtures were set aside for 30 min to accomplish thermal equilibrium and to allow any bubbles developed during the stirring process to rise to the surface before the blends were stable and ready for testing. Afterwards, the physical-chemical properties of the fuel samples were measured via the ASTM standard test methods.



Figure 2. Fuel samples; from the right N100, N75, N50, N25, and DF.

Table 1. Naming of the diesel fuel-HILO blends.

Fuel	HILO (vol.%)	Diesel Fuel, DF (vol.%)
N0	0	100
N25	25	75
N50	50	50
N75	75	25
N100	100	0

2.2. Chemical Composition

The chemical compositions of *Hermetia illucens* larvae oil were identified using an EQPCL 173 Agilent 6890A (G1530A) (Agilent Technologies, Santa Clara, CA, USA) gas chromatography (GC) system. The gas chromatography-mass spectrometry (GC-MS) scientific technique was executed using the gas carrier of helium through an initial flow of 1.0 mL/min. The GC-MS comes with an analytical capillary column model number Agilent 19091s-433 with a maximum temperature of 325 °C (HP-5MS, 0.25 µm nominal film thickness, 250.00 µm nominal diameter, and 30.0 m nominal length). The column settings were set under constant flow with an average velocity of 29 cm/s, the nominal initial pressure of 16.93 psi (116.73 kPa), and an initial flow of 1.0 mL/min. The front detector of the GC-MS was fitted out with Agilent thermal conductivity detector (TCD) with a temperature of 250 °C, a universal detector that responds to all compounds, excluding the gas carrier. The oven temperature was firstly maintained at 150 °C for about one minute, then heated to 340 °C of maximal temperature. The finding in output spectra was compared with the National Institute of Standards and Technology (NIST) mass spectral library for chemical compounds identification [38].

2.3. CHNOS Elements

The EQPCL 200 Vario MACRO cube: Elemental Analyzer (Elementar, Langensfeld, Germany) was used to measure the amount of element CHNOS (carbon content, C; hydrogen content, H; nitrogen content, N; oxygen content, O; and sulfur content, S) in the HILO and diesel fuel blends. The oxygen content of the fuel was computed using Equation (1) [39,40]. All of the measurements were carried out strictly according to the ASTM D5291 and ASTM D5373 standards.

$$\text{Oxygen, } O\% = 100 - (C\% + H\% + N\% + S\% + \text{Ash}\%) \quad (1)$$

where C is carbon content, H is hydrogen content, N is nitrogen content, O is oxygen content, and S is sulfur content.

2.4. Density

Density was measured following the ASTM D4052 standard. According to this standard, density is determined at the existing temperature and corrected to 15 °C using a series of calculations and international standards tables. The testing device used was a Kyoto Electronics Manufacturing (KEM) Density/Specific Gravity Meter (model DA-640), (Kyoto Electronics Manufacturing Co., Ltd., Kyoto, Japan). The density value was measured using a minimum amount of 1.0 mL test fuel inserted into a temperature-controlled sample cell. The density of the test fuel is computed using Equation (2): the measurement for each sample was repeated three times with acceptable repeatability, and the averaged values were considered the final results.

$$\rho = A \cdot p^2 - B \quad (2)$$

where ρ is density (kg/m^3), A and B are cell constants measured from oscillation frequencies once the cell is filled up with calibration fluid of identified density, p is period (s) = $1/f$ and f is oscillation frequency.

2.5. Viscosity

Kinematic viscosity was determined following the ASTM D445 standard. It is defined as a fluid's resistance to flow when no external force is exerted, except under gravity influence at 40 °C. It involves the time determining for a specified volume of fluid to flow under gravity influence through a capillary at an identified and carefully controlled temperature. The measurement equipment was a calibrated Cannon-Fenske Routine Viscometer and a Cole-Parmer Polystat economical constant temperature bath at 40 ± 0.05 °C. The Cannon-Fenske Routine Viscometer sizes No. 100 and No. 150, with a viscosity range of 3.0–15.0 mm^2/s and 7.0–35.0 mm^2/s , respectively, were used in this study. The kinematic viscosity, v (mm^2/s), is computed using Equation (3):

$$v = C_v \cdot t \quad (3)$$

where C_v is viscometer calibration constant (mm^2/s^2) and t is measured flow time, s . The calibration constant, C_v , is supplied by a local Cannon-Fenske Routine Viscometer supplier, where it is equivalent to 0.015 mm^2/s and 0.035 mm^2/s for the viscometer size No. 100 and No. 150, respectively.

2.6. Heating Value

The heating value of fuel samples was determined according to the ASTM D240 standard. The testing equipment used was the Parr 6772 Calorimetric Thermometer, (Parr Instrument Company, Moline, IL, USA) with the oxygen bomb calorimeter. During the calorimetric pre-period, the equipment precisely determined heat leak. These measured values are the actual surrounding temperature of the calorimeter. The values are utilized over the testing period as a correction constant for the calorimeter heat leak. It makes use of the controller ability without any supplementary expenses. The purpose is to develop

heat leak correction ability comparable to the method applied when manual calorimetric and non-electronic thermometry approaches were used.

2.7. Cetane Number

The cetane numbers of the fuel samples were measured following the ASTM D613 standards using a Shatox SX-100M, (SHATOX Co., LLC, Tomsk, Russia), portable octane/cetane analyzer. The fuel quality analyzer is developed to evaluate the cetane and octane numbers of fuel. It is suitable for laboratory and field conditions and is designed to operate at air temperatures of $-10\text{ }^{\circ}\text{C}$ up to $45\text{ }^{\circ}\text{C}$. The operation principle of the analyzer is discovering the self-flammability of diesel fuel and knocks characteristics of gasoline using a detector. The detector is a 75 mL non-separable container. Its specific volume identifies the signal features produced from a sensor located at the detector base. The detector is also equipped with an integrated component sensitive to temperature variations of the fuel sample. A separate imitator is provided with the detector to check the equipment performance without using any fuel samples. The electronic calculator inside the analyzer processed the detector's signals. It also performs all essential calculations and continuously monitors the primary function of the analyzer.

2.8. Flash Point

The ASTM D93 standard was used to determine the flash point of certain test fuels. The testing equipment used was a Koehler rapid flash point tester (closed cup, small scale flash point tester). It is suitable for environmental compliance testing and quality assurance and the actual flash point for hydrocarbons, fragrances, paints, and other liquids. A flash or no flash result is obtained in one minute using a minimum of a 2 mL sample for flash points below $100\text{ }^{\circ}\text{C}$. The temperature was set using the digital display controller, and a sample of about 2 mL or 4 mL was injected into the sample cup. The tester rapidly became stable at the pre-set temperature value, allowing the test flame to be applied and the result to be observed. The measurement for each sample was carried out no less than three times with acceptable repeatability to ensure an accurate outcome.

3. Results and Discussion

The physical-chemical properties of neat HILO and diesel fuel are important in determining the engine combustion, performance, and exhaust emissions characteristics. Therefore, these properties must be presented before further analysis of the blended fuels. These properties are important to understand each test fuel's character before relating them to any finding. Determining and formulating the influence of the increasing ratio of HILO in the fuel blends is critical to describe the trend of the individual fuel property. Neat HILO (N100) was mixed by volume ratio with diesel fuel at 25% incremental, and the test fuels applied in this research consist of pure diesel fuel (N0), N25, N50, N75, and neat HILO (N100). The test fuel properties consist of the chemical composition, CHNOS elements, density, viscosity, heating value, cetane number, and flash point. All fuel properties measurements were carried out strictly following the ASTM standard methods. The measured fuel properties of the test fuels are presented in Table 2.

Table 2. Measured the physical-chemical properties of the test fuels.

Properties	ASTM D975		Error	DF	DF-HILO Blends			HILO
	Standard	Limits			N0	N25	N50	
Density at $15\text{ }^{\circ}\text{C}$ (kg/m^3)	D4052	-	0.50	829.00	869.48	885.84	902.11	922.53
Kinematic viscosity (mm^2/s)	D445	1.9–4.1	0.05	3.35	7.52	11.47	19.81	28.15
Heating value (MJ/kg)	D240	-	0.35	48.115	45.913	43.537	41.542	40.836
Cetane number	D613	Min. 40	0.50	52	55.9	59.2	60.8	61
Flash point ($^{\circ}\text{C}$)	D93	Min. 52	9.00	60	90	98	112	399

Table 2. Cont.

Properties	ASTM D975		Error	DF	DF-HILO Blends				HILO
	Standard	Limits			N0	N25	N50	N75	
Element C (wt.%)	-	-	0.01	87.17	83.49	81.61	78.43	76.44	
Element H (wt.%)	-	-	0.01	12.76	13.11	13.31	13.62	13.77	
Element N (wt.%)	-	-	0.01	0.07	0.12	0.21	0.27	0.31	
Element O (wt.%)	-	-	0.01	0	3.25	4.82	7.62	9.39	
Element S (wt.%)	-	-	0.01	0	0.03	0.05	0.06	0.09	

3.1. Chemical Composition of HILO and Diesel Fuel

A gas chromatography-mass spectrometry was utilized to detect, quantify, and identify the chemical compositions in HILO. All of the findings were compared with the baseline diesel fuel. The function of GC-MS was to provide detailed information on the chemical composition of diesel fuel and HILO. The gas chromatogram produces a peak graph representing each chemical compound detected in the fuel. The number of peaks indicates the number of separated chemical compositions in the fuel samples. The position of the individual peaks represents the retention time of individual chemical composition.

The chromatograms for diesel fuel and HILO are shown in Figures 3 and 4, respectively. Based on both figures, the chemical compositions of diesel fuel had been traced at the early beginning of the retention time, and the process was almost complete at the half retention time of 27.00 min. However, the scenario for HILO is different. The chemical composition of HILO starts to be traced about the middle retention time of 19.00 min and is almost complete at the end of the retention time (minute of 51.00). In addition, both trends can be easily understood as the chemical composition of diesel fuel was detected at the beginning of the retention time. In contrast, the chemical composition of HILO was detected at the end of the retention time. Therefore, the early detection chemical composition of the diesel fuel shows that diesel fuel contains high volatility chemical compounds.

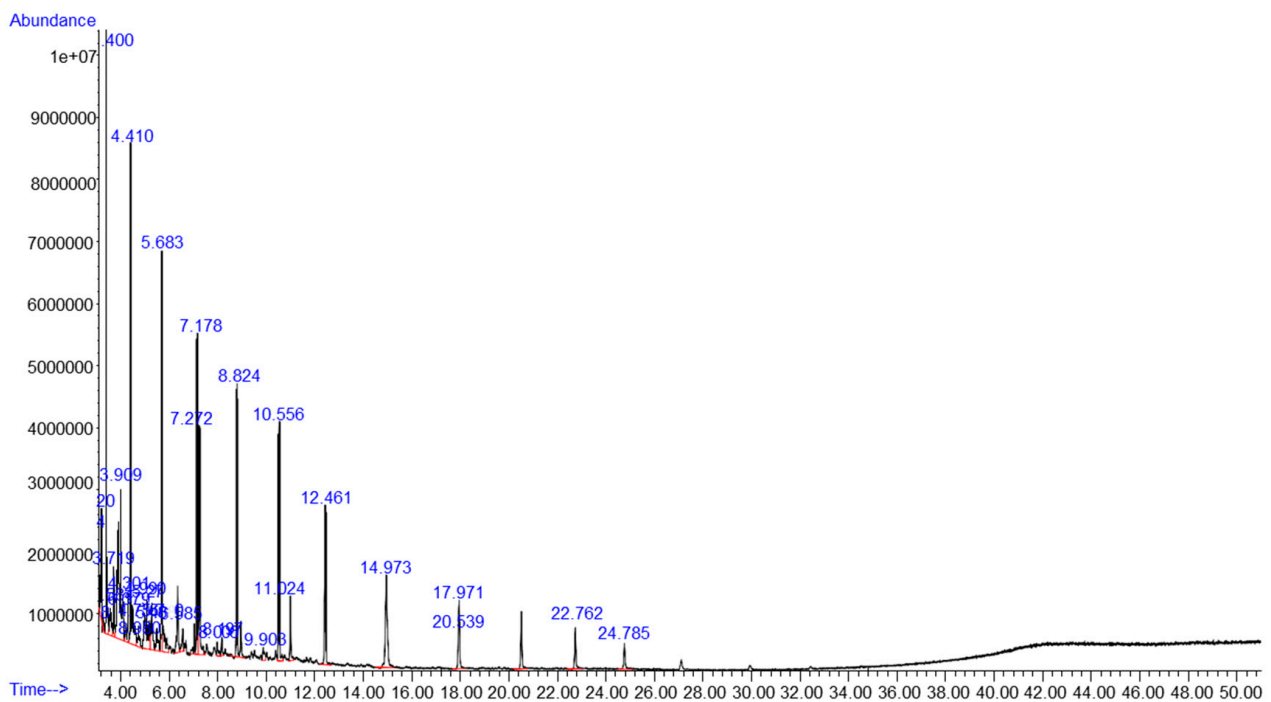


Figure 3. Gas chromatogram of diesel fuel.

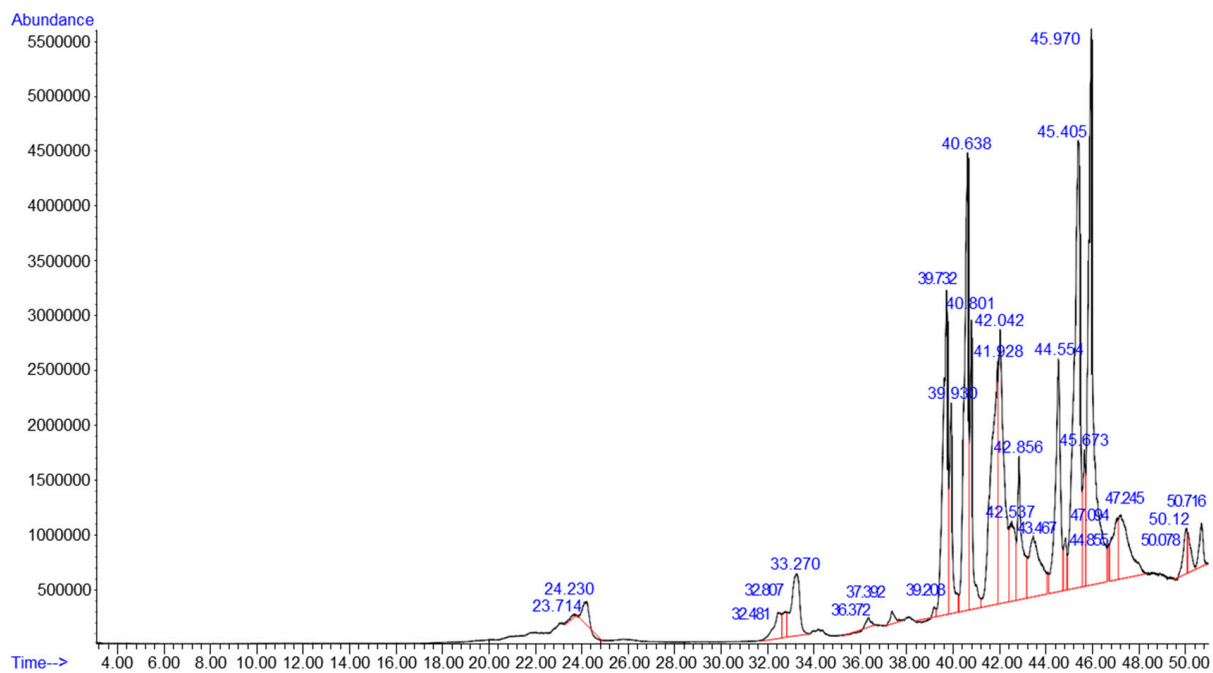


Figure 4. The GC chromatogram of HILO.

On the other hand, the late detection chemical compound of HILO indicates that HILO contains a chemical compound with low volatility characteristics. The volatility of the chemical compound will directly influence the flash point of the individual fuel. Moreover, Misra, et al. [41] reported that most volatile compounds are low molecular weight. This statement is consistent with the mass spectrometer findings of diesel fuel, which is more volatile than HILO due to its low molecular weight compound.

The chemical compositions of the diesel fuel and HILO were determined from the peak of chromatograms. The mass spectrum data identified them as tabulated in Table A1 (Appendix A) and Table A2 (Appendix B), respectively. Table 3 summarized the chemical composition of diesel fuel and HILO determined in this study. Based on the mass spectrometer findings, diesel fuel was composed of various hydrocarbons with varying chain lengths. The primary chemical composition in the diesel fuel is made up of 73.3095 wt.% paraffin (alkane) of volatile compounds. Aromatics comprised 22.085 wt.% of the volatiles, while carboxylic acids accounted for 2.9747 wt.%. An olefin series total for 1.6309 wt.%. The high content of the alkane hydrocarbon family in the diesel fuel is remarkable compared to the remaining family of the hydrocarbon compound. On the other hand, HILO was composed of almost different chemical compositions than diesel fuel. HILO predominantly consisted of 95.113 wt.% carboxylic acids (fatty acids) of volatiles compounds. Ketones content was 0.0771 wt.% and other compounds accounted for 4.8097 wt.% of volatiles. Therefore, the mass spectrometer findings indicated that carboxylic acid was the dominant species for the HILO compound.

Table 3. Summary of the chemical compound in diesel fuel and HILO.

Hydrocarbon Family	Diesel Fuel (wt.%)	HILO (wt.%)
Paraffin (alkane)	73.3095	-
Olefins (alkenes)	1.6309	-
Aromatics	22.085	-
Carboxylic acids (fatty acids)	2.9747	95.113
Ketones	-	0.0771
Others	-	4.8097
	100.0001	99.9998

In general, the energy content of a certain fuel also can be predicted based on its hydrocarbon chain length. An increase in hydrocarbon chain length leads to an increase in energy density, boiling point, and decrease in volatility [42]. Conversely, fuel with normal alkane hydrocarbon has the highest ignition quality, increasing chain length. According to the gas chromatography results, the diesel fuel was made up of predominantly paraffin (alkane) and aromatic families. The presence of the alkane family in diesel fuel made the diesel fuel have very good ignition quality. Furthermore, the aromatic family's existence contributes to high energy content per unit volume of diesel fuel [43]. Nevertheless, HILO properties are expected to reduce ignition quality and lower energy content due to the absence of alkane and aromatic compounds.

In addition, the number of atoms in the molecular structure plays an important role in determining the boiling temperature of the fuel. The boiling temperature increases as the number of atoms in the molecular structure increases. Therefore, fuels with fewer numbers of atoms in the molecule structure tend to be more volatile [44]. Referring to the chemical composition of diesel fuel and HILO, it was observed that the predominant alkane hydrocarbon in the diesel fuel varies between 14–32 numbers of carbon atoms. While HILO mainly consists of dodecanoic acid, 1,2,3-propanetriyl ester consists of 39 carbon atoms. Therefore, the lower number of atoms in the diesel fuel leads to lower boiling temperature and more volatility. On the other hand, due to the higher number of atoms in the molecular structure of HILO, the boiling temperature and volatility are expected to be higher in temperature and less volatile.

The proportions of hydrogen atoms to carbon atoms also directly relate to heating value. The heating value normally increases as the proportion of hydrogen atoms to carbon atoms in the molecule increases due to the higher heating value of hydrogen than carbon [45]. Based on the results, diesel fuel has a higher proportion of hydrogen atoms to carbon atoms than HILO. Thus, diesel fuel has a higher heating value than HILO.

3.2. Influence of HILO on Density

The density of diesel fuel-HILO blends used in the present study was observed between 829.00 kg/m³ to 922.53 kg/m³, as tabulated in Table 2. The fuel density with various volume percentages of biofuel in the fuel mixture is shown in Figure 5. Adding HILO to the fuel mixture further increases the fuel blend density, resulting in the fuel blend densities marginally higher than those of the diesel fuel. According to Atabani, et al. [46], the density of biofuel is influenced by the raw material used in the production process. Therefore, the density of the fuel blends increases with increasing HILO concentration in the mixture due to the blending effect with the HILO. It is mainly due to the density of HILO, which is substantially 11.28% heavier than diesel fuel. In addition, the difference in density between the diesel fuel and the blended fuels of N25, N50, and N75 are 4.88%, 6.86%, and 8.82%, respectively, higher when compared to diesel fuel. Altıparmak, et al. [47] also discovered that the density of diesel fuel-tall oil methyl ester blends increased with biodiesel. Based on Figure 5, the density position of diesel fuel-HILO blends are almost similar with reported by Altıparmak, Keskin, Koca and Gürü [47] and Pramanik [48] when using biodiesel of tall oil and neat *Jatropha curcas* oil, respectively. This shows that even the density of diesel fuel-HILO blends is similar with the tall oil used Altıparmak, Keskin, Koca and Gürü [47] which already converted into biodiesel. As the biodiesel process will lowering the density of biofuel. Therefore, the densities of diesel fuel-HILO blends are expected to be much lower when using HILO which already converted into biodiesel form. In the other hand, finding reported by Kwanchareon, et al. [49] and Mofijur, et al. [50] when using biodiesel of palm oil and *Moringa oleifera*, respectively, indicates lower densities trend as compared to the diesel fuel-HILO blends. Moreover, Torres-Jimenez, et al. [51] claimed that an increase in density caused an advanced injection timing, which could contribute to a significant deterioration of engine performance as well as an increase in exhaust emission pollution. This limitation can be solved by modifying the injection timing [52].

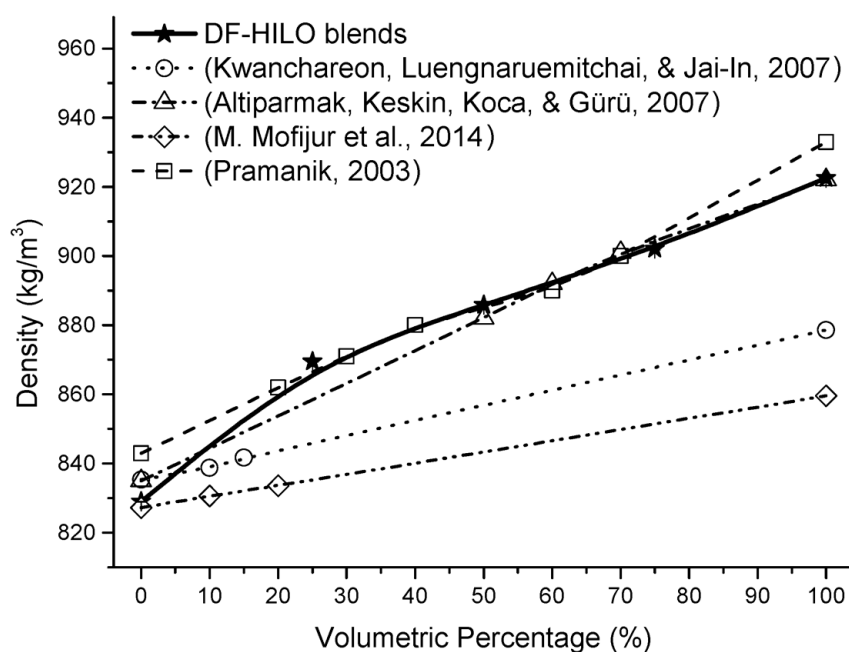


Figure 5. Densities of DF-HILO fuel blends [47–50].

3.3. Influence of HILO on Viscosity

The kinematic viscosities of diesel fuel-HILO blends vary in the range of 7.52 mm²/s to 19.81 mm²/s, and the average kinematic viscosity value for HILO is 28.15 mm²/s, which is higher than those of the baseline diesel fuel (3.35 mm²/s) as shown in Table 2. Kinematic viscosities of the diesel fuel-HILO blends against volumetric percentages are presented in Figure 6. It was observed that the viscosity of the fuel blends increases as the HILO volume percentage increases in the fuel mixture. Adding HILO further increases the kinematic viscosity due to the higher viscosity of HILO compared to diesel fuel. Based on the analysis, the highest density is denoted by HILO, whereas the kinematic viscosity of the blended fuels of N25, N50, and N75 is 124.48%, 242.39%, and 491.34%, respectively, are higher than the diesel fuel owing to the blending effect with HILO. Similar to density, the diesel fuel-HILO blends' kinematic viscosity is in agreement with the earlier investigation by Pramanik [48] that observed the kinematic viscosity of diesel fuel-jatropha curcas oil blends increases with the addition of jatropha curcas oil in the fuel mixture. However, the author finding on kinematic viscosity is much higher than the diesel fuel-HILO blends. This trend reveals that HILO has bright potential to be one of the future alternative fuels. In the other hand, finding by Altiparmak, Keskin, Koca and Gürü [47], Raheman and Phadataré [53], and Mofijur, Masjuki, Kalam, Atabani, Arbab, Cheng and Gouk [50] when using biodiesel of tall oil, karanja methyl ester, and Moringa oleifera shows lower kinematics viscosities than HILO due to the biofuel used had been treated to improve its properties. As the diesel fuel-HILO blends increase by HILO addition, the fuel atomization is expected to be marginally worsened and directly reduce the engine power.

3.4. Influence of HILO on Heating Value

The heating value for HILO, diesel fuel, and its fuel blends are presented in Table 2. Based on the results, the lowest heating value is recorded by HILO at 40.836 MJ/kg, which is 15.13% lower than the diesel fuel at 48.115 MJ/kg. It is due to the chemical composition of HILO, which contains oxygen elements in the structure. The oxygen content is not a common element in diesel fuel. In addition, the lower carbon content in HILO contributes to a lower heating value than diesel fuel. This finding agrees with Demirbas [54], which reported that biofuels have different heating values, mainly depending on biofuel feedstock. Normally, biodiesel produced from biofuel feedstock has a lower heating value of about 10% to 15% than diesel fuel.

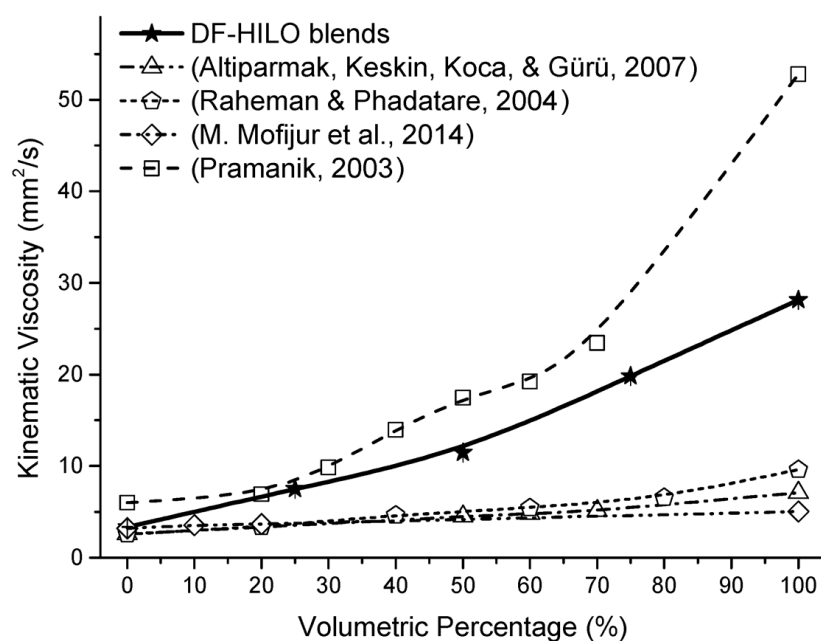


Figure 6. Kinematic viscosity vs. volumetric percentage [47,48,50,53].

The heating value curves against the different concentrations of biofuel are presented in Figure 7. It can be seen that the heating value of the diesel fuel-HILO blends decreases significantly with the addition of HILO. This behavior is a result of the lower heating value of HILO compared to diesel fuel. Additionally, the heating value of the fuel blends of N25, N50, and N75 is lower than that of diesel fuel by 4.58%, 9.51%, and 13.66%, respectively, due to the blending effect with HILO. This result is in line with earlier literature by Kwanchareon, Luengnaruemitchai and Jai-In [49] that found the heating value of the fuel blends reduced with the addition of palm oil biodiesel. Based on the figure, diesel fuel-HILO blends contains advantage in higher heating value than the biofuels used by other researchers [47–50]. Moreover, the low heating value of fuel has a direct influence on the power output of the engine.

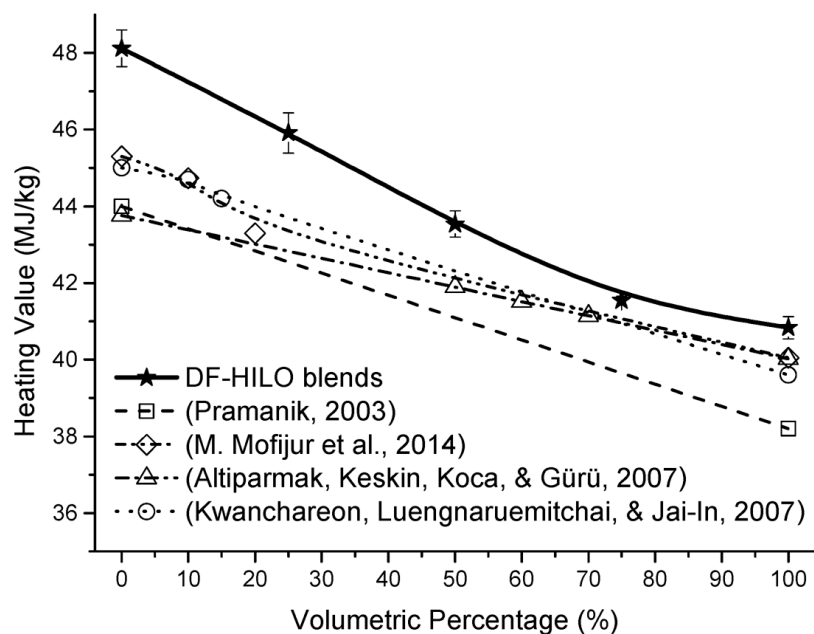


Figure 7. Variation of heating value with volumetric percentage [47–50].

3.5. Influence of HILO on Cetane Number

Table 2 shows that the cetane numbers of diesel fuel-HILO blends vary in the range of 55.9 to 60.8, and the highest cetane number of 61 is recorded by neat HILO, which is higher than the diesel fuel with a cetane number of 52. The higher cetane number of HILO can be attributed to the main component in the HILO composition. It was observed that HILO consists of higher saturated fatty acid acting as the key element in the fuel composition. It also contains higher oxygen content which affects in higher cetane number compared to diesel fuel. The present finding is also supported by various studies [55–57], which concluded that most biofuels have a higher cetane number than diesel fuel, as biofuels are mainly composed of long-chain hydrocarbon groups.

Furthermore, Mosarof, et al. [58] and Bhuiya, et al. [59] reported that higher saturated fatty acid and oxygen content in the fuel composition are also the factors that contribute to the higher cetane number of biofuels. The higher cetane number of HILO and its blends may cause shorter ignition delay, resulting in less fuel taking part during premix combustion duration, while more fuel burned during diffusion combustion duration. This condition leads to decreasing in the in-cylinder rate of pressure rise, which may contribute to lower in-cylinder temperature.

Figure 8 presents the cetane number curve against the volumetric percentage of fuel blends. It can be observed that the cetane number of the diesel fuel-HILO blends increases significantly with increasing the volumetric percentage of the HILO in the fuel mixture. This trend is due to the 17.31% higher cetane number of HILO than diesel fuel. The cetane number of fuel blends for N25, N50, and N75 are 7.5%, 13.85%, and 16.92% higher than the diesel fuel, respectively. The findings are consistent with previous research by Alptekin and Canakci [60], which involves two types of diesel fuels mixed with five edible vegetable oils: cottonseed, corn, canola, soybean, and sunflower oil. The cetane number value of diesel fuel-HILO blends are almost similar to Alptekin and Canakci [60], but much more higher than biodiesel used by Mofijur, Masjuki, Kalam, Atabani, Arbab, Cheng and Gouk [50], Altıparmak, Keskin, Koca and Gürü [47], and Kwanchareon, Luengnaruemitchai and Jai-In [49]. These condition is might due to both biofuels of HILO and five edible vegetable oils by Alptekin and Canakci [60] are in neat or pure biofuel form. Therefore, the cetane number of HILO is expected to reduce when converted into biodiesel form.

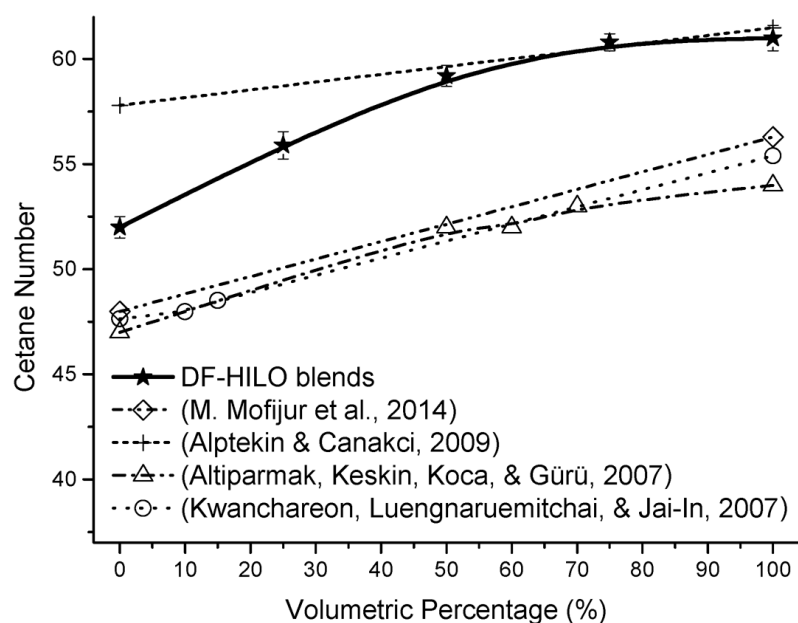


Figure 8. Variation in cetane number with volumetric percentage (vol.%) [47,49,50,60].

3.6. Influence of HILO on Flash Point

Figure 9 illustrates the flash point curve of the blended fuels with different biofuel concentrations in the fuel mixture. It exposes that adding HILO to the fuel mixture further increases the flash point of the diesel fuel-HILO blends. According to Table 2, the flash points of diesel fuel-HILO blends are between 90 °C to 112 °C, which is higher than diesel fuel. For this reason, the flash points of the blends are slightly higher than the diesel fuel due to the flash point of HILO, which is greatly higher than the diesel fuel. The flash point of fuel blends for N25, N50, and N75 are 50%, 63.33%, and 86.67%, respectively, which are higher than diesel fuel due to blending with HILO.

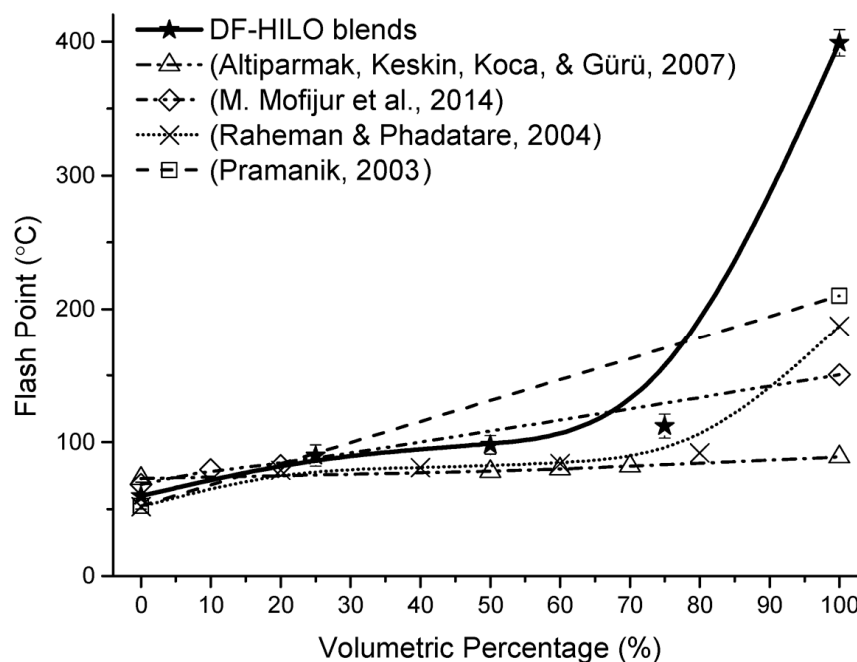


Figure 9. Variation in flash point with volumetric percentage (vol.%) [47,48,50,53].

The flash point does not vary significantly for the N25 blend of HILO. It owes to the diesel fuel compositions, creating the combustible vapor that formed a similar temperature to the neat diesel fuel [61]. On the other hand, the flash points rise remarkably for the blends containing 50% and 75% of HILO. This is a result of biofuel's greater flash point than diesel fuel's. It was observed that the flash point was influenced by the most volatile element (diesel fuel) in the present study. Diesel fuel evaporates firstly during the heating process. Therefore, the start of ignition is observed around this temperature for most of the fuel blends comprising biofuel that is lower than 25%. Various researchers have reported that flash point increases significantly with biofuel introduction, especially for fuel blends comprising neat oil or biodiesel [53]. As referring to the figure, the flash points of diesel fuel-HILO blends for N25, N50, and N75 are almost similar to findings reported by Altiparmak, Keskin, Koca and Gürü [47], Mofijur, Masjuki, Kalam, Atabani, Arbab, Cheng and Gouk [50], Raheman and Phadataré [53], and Pramanik [48] when using biodiesel of tall oil, Moringa oleifera, karanja methyl ester, and neat jatropha curcas oil, respectively.

4. Conclusions

In the present work, it has been revealed that diesel fuel-HILO blends' physical and chemical properties provide important information about their behaviour as fuel for diesel engines. In common terms, it can be summarized that the investigated diesel fuel-HILO blends indicate an equivalent fuel properties value to the diesel fuel. The chemical composition of the diesel fuel and HILO were observed through GC-MS analysis. The carbon composition of HILO is generally 12.31% lesser than that of diesel fuel. Therefore, adding HILO into the diesel fuel reduced the carbon composition in the fuel blends, causing

a slight decrease (15.13%) in the energy content. Furthermore, the increment in oxygen content (in the diesel fuel-HILO blends) is predicted to have a valuable influence on the exhaust emissions characteristics compared with the direct utilization of diesel fuel and improve the combustion efficiency.

Density and kinematic viscosity of the test fuel blends were increased (11.28% and 740.30%, respectively) by the introduction of HILO. The increases in density and viscosity also parallel with findings reported by Altıparmak, Keskin, Koca and Gürü [47] and Pramanik [48] when using tall oil methyl ester and jatropha curcas oil, respectively. In addition, due to the low volatility of HILO, the common problems related to diesel fuel storage may not occur. However, the low volatility affects injection timing, ignition, and combustion characteristics. Besides the fact that the heating value of fuel blends reduces by 13.66% than that of diesel fuel, adding HILO increases the cetane number up to 16.92%. It is essential to perceive that flash points will indicate the volatility value of the chemical compound. Since the HILO consists of a less volatile compound, therefore the flash point of HILO blends is 50–86.67% higher than the diesel fuel. Kwanchareon, Luengnaruemitchai and Jai-In [49] and Alptekin and Canakci [60] also reported the similar finding when dealing with various biofuels such as palm oil, cottonseed, corn, canola, soybean, and sunflower oil.

Author Contributions: Conceptualization, M.K.K., A.A., S.H., D.R. and K.K.; methodology, M.K.K. and A.A.; validation, M.K.K. and A.A.; formal analysis, M.K.K.; M.S.—investigation, M.K.K. and S.H.; data curation, M.K.K.; writing—original draft preparation, M.K.K.; S.S., writing—review and editing, M.K.K.; T.Y.—visualization, M.K.K. and A.A.; supervision, A.A.; project administration, A.A.; funding acquisition, A.A. and D.R. All authors have read and agreed to the published version of the manuscript.

Funding: This research was funded by the MINISTRY OF HIGHER EDUCATION (MALAYSIA), the University Malaysia Pahang Fundamental Research Grant Scheme (FRGS) RDU1901153 and FRGS/1/2018/TK03/UMP/02/26 RDU 190194.

Data Availability Statement: Not applicable.

Acknowledgments: The authors sincerely thank the Ministry of Higher Education (Malaysia) for financial support through the MyBrain15 program and the University Malaysia Pahang Fundamental Research Grant Scheme (FRGS) RDU1901153 and FRGS/1/2018/TK03/UMP/02/26 RDU 190194. “Mohd Kamal bin Kamarulzaman” is the recipient of the UMP Post-Doctoral Fellowship in Research.

Conflicts of Interest: The authors declare no conflict of interest.

Appendix A

Table A1. Chemical composition of diesel fuel.

No.	Compound Name	Structure/ Shorthand	Formula	Molar Mass (g/mol)	Hydrocarbon Family	Saturated/ Unsaturated	Stability	DF (wt.%)
1	Naphthalene, 1,6-dimethyl-	C12:5	C ₁₂ H ₁₂	156.22	Aromatics	Highly unsaturated	Most unstable	10.0334
2	Pentadecane	C15:0	C ₁₅ H ₃₂	212.421	Paraffin	Saturated	Stable	9.4548
3	Tetradecane	C14:0	C ₁₄ H ₃₀	198.39	Paraffin	Saturated	Stable	8.7604
4	Heptadecane	C17:0	C ₁₇ H ₃₆	240.5	Paraffin	Saturated	Stable	7.7215
5	Hexadecane	C16:0	C ₁₆ H ₃₄	226.44	Paraffin	Saturated	Stable	7.3136
6	Octadecane	C18:0	C ₁₈ H ₃₈	254.5	Paraffin	Saturated	Stable	6.2162
7	Pentadecane, 2,6,10,14-tetramethyl-	C19:0	C ₁₉ H ₄₀	268.5	Paraffin	Saturated	Stable	6.194
8	Nonadecane	C19:0	C ₁₉ H ₄₀	268.5	Paraffin	Saturated	Stable	5.7505
9	Eicosane	C20:0	C ₂₀ H ₄₂	282.5	Paraffin	Saturated	Stable	4.8809
10	Heneicosane	C21:0	C ₂₁ H ₄₄	296.6	Paraffin	Saturated	Stable	4.8401
11	Naphthalene, 1,6,7-trimethyl-	C13:5	C ₁₃ H ₁₄	170.25	Aromatics	Highly unsaturated	Most unstable	3.8814
12	Eicosane	C20:0	C ₂₀ H ₄₂	282.5	Paraffin	Saturated	Stable	2.4984
13	Pentadecane, 2,6,10-trimethyl-	C18:0	C ₁₈ H ₃₈	254.5	Paraffin	Saturated	Stable	2.1935
14	Docosane, 11-decyl-	C32:0	C ₃₂ H ₆₆	450.9	Paraffin	Saturated	Stable	1.897
15	Dodecane, 2,6,11-trimethyl-	C15:0	C ₁₅ H ₃₂	212.41	Paraffin	Saturated	Stable	1.7759

Table A1. Cont.

No.	Compound Name	Structure/ Shorthand	Formula	Molar Mass (g/mol)	Hydrocarbon Family	Saturated/ Unsaturated	Stability	DF (wt.%)
16	Anthracene, 1,2,3,4-tetrahydro-	C14:5	C ₁₄ H ₁₄	182.266	Aromatics	Highly unsaturated	Most unstable	1.737
17	17-Pentatriacontene	C35:1	C ₃₅ H ₇₀	490.9	Olefins	Unsaturated	Unstable	1.6309
18	Pentadecanoic acid, 14-methyl-, methyl ester	C17:0	C ₁₇ H ₃₄ O ₂	270.5	Carboxylic acids	Saturated	Very stable	1.6144
19	Naphthalene, 1,4,6-trimethyl-	C13:5	C ₁₃ H ₁₄	170.25	Aromatics	Highly unsaturated	Most unstable	1.3927
20	11,12-Dibromo-tetradecan-1-ol acetate	C16:0	C ₁₆ H ₃₀ Br ₂ O ₂	414.2	Carboxylic acids	Saturated	Very stable	1.3603
21	Tricosane	C23:0	C ₂₃ H ₄₈	324.6	Paraffin	Saturated	Stable	1.3463
22	Decahydro-4,4,8,9,10-pentamethylnaphthalene	C15:0	C ₁₅ H ₂₈	208.38	Aromatics	Highly unsaturated	Most unstable	1.3274
23	Naphthalene, 1,5-dimethyl-	C12:5	C ₁₂ H ₁₂	156.22	Aromatics	Highly unsaturated	Most unstable	1.2802
24	Nonacosane	C29:0	C ₂₉ H ₆₀	408.8	Paraffin	Saturated	Stable	1.0636
25	Naphthalene, 1,4,5-trimethyl-	C13:5	C ₁₃ H ₁₄	170.25	Aromatics	Highly unsaturated	Most unstable	1.0588
26	Tetracosane	C24:0	C ₂₄ H ₅₀	338.7	Paraffin	Saturated	Stable	0.8935
27	Naphthalene, 1,6,7-trimethyl-	C13:5	C ₁₃ H ₁₄	170.25	Aromatics	Highly unsaturated	Most unstable	0.8599
28	Benzene, (4,5,5-trimethyl-1,3-cyclopentadien-1-yl)-	C14:5	C ₁₄ H ₁₆	184.28	Aromatics	Highly unsaturated	Most unstable	0.5142
29	Octadecane, 1-(ethenyl-oxo)-	C20:0	C ₂₀ H ₄₀ O	296.5	Paraffin	Saturated	Stable	0.5093 100.0001

Appendix B

Table A2. Chemical composition of HILO.

No.	Compound Name	Structure/ Shorthand	Formula	Molar Mass (g/mol)	Hydrocarbon Family	Saturated/ Unsaturated	Stability	HILO (wt.%)
1	Dodecanoic acid, 1,2,3-propanetriyl ester	C39:0	C ₃₉ H ₇₄ O ₆	639.00	Carboxylic acids	Saturated	Very stable	74.051
2	3-[7-Bromo-5-(2-chloro-phenyl)-2-oxo-2,3-dihydro-1H-benzo[e][1,4]diazepin-3-ylamino]-benzoic acid	-	C ₁₉ H ₁₄ BrClN ₂ O ₅	465.7	Carboxylic acids	Saturated	Very stable	13.858
3	Indole-3-carboxylic acid, 1-benzyl-5-methoxy-2-methyl-, ethyl ester	-	-	-	Carboxylic acids	-	-	3.6025
4	Aprobarbital, bis(trimethylsilyl)-Carbamic acid,	-	-	-	-	-	-	3.4296
5	N-(3-chloro-4-methoxyphenyl)-, glycidyl ester	-	C ₁₀ H ₁₂ ClNO ₂	213.66	Carboxylic acids	Saturated	Very stable	2.6763
6	Lauric anhydride	C24:0	C ₂₄ H ₄₆ O ₃	382.6	Carboxylic acids	Saturated	Very stable	0.9252
7	N-Trifluoroacetyl demecolcine	-	C ₂₃ H ₂₄ F ₃ NO ₆	467.4	-	-	-	0.6915
8	Iron, cyclopentadienyl-ethyl-1,2-diisopropylphosphinoethane	-	C ₂₁ H ₄₄ FeP ₂ +6	414.4	-	-	-	0.6359
9	Trans-4'-Dimethylamino-4-(methylthio)chalcone	-	C ₁₇ H ₁₇ NO	251.32	Ketones	-	-	0.0771
10	Aluminum, bis(2-methylpropyl)(2,4-pentanedionato-O,O')-, (T-4)-	-	-	-	-	-	-	0.0527 99.9998

References

- Kalu-Uka, G.M.; Kumar, S.; Kalu-Uka, A.C.; Vikram, S.; Okorafor, O.O.; Kigozi, M.; Ihekwe, G.O.; Onwualu, A.P. Prospects for biodiesel production from *Macrotermes nigeriensis*: Process optimization and characterization of biodiesel properties. *Biomass Bioenergy* **2021**, *146*, 105980. [[CrossRef](#)]
- Kadrigama, G.; Kamarulzaman, M.K.; Ramasamy, D.; Kadrigama, K.; Hisham, S. Classification of Lubricants Base Oils for Nanolubricants Applications—A Review. In *Technological Advancement in Mechanical and Automotive Engineering*; Springer: Singapore, 2023; pp. 205–213.
- De Oliveira, A.; Valente, O.S.; Sodré, J.R. Effects of ethanol addition to biodiesel-diesel oil blends (B7 and B20) on engine emissions and fuel consumption. *MRS Adv.* **2017**, *2*, 4005–4015. [[CrossRef](#)]
- Ali, M.H.; Adam, A.; Yasin, M.H.M.; Kamarulzaman, M.K.; Othman, M.F. Mitigation of NO_x emission by monophenolic antioxidants blended in POME biodiesel blends. *Greenh. Gases Sci. Technol.* **2020**, *10*, 829–839. [[CrossRef](#)]

5. Mihankhah, T.; Delnavaz, M.; Khaligh, N.G. Application of TiO₂ nanoparticles for eco-friendly biodiesel production from waste olive oil. *Int. J. Green Energy* **2018**, *15*, 69–75. [[CrossRef](#)]
6. Bakar, R.; Kadirgama, K.; Ramasamy, D.; Yusaf, T.; Kamarulzaman, M.; Aslfattahi, N.; Samylingam, L.; Alwayzy, S.H. Experimental analysis on the performance, combustion/emission characteristics of a DI diesel engine using hydrogen in dual fuel mode. *Int. J. Hydrogen Energy* **2022**. [[CrossRef](#)]
7. Singh, D.; Sharma, D.; Soni, S.; Inda, C.S.; Sharma, S.; Sharma, P.K.; Jhalani, A. A comprehensive review of physicochemical properties, production process, performance and emissions characteristics of 2nd generation biodiesel feedstock: *Jatropha curcas*. *Fuel* **2021**, *285*, 119110. [[CrossRef](#)]
8. Singh, D.; Sharma, D.; Soni, S.; Sharma, S.; Sharma, P.K.; Jhalani, A. A review on feedstocks, production processes, and yield for different generations of biodiesel. *Fuel* **2020**, *262*, 116553. [[CrossRef](#)]
9. Aransiola, E.; Ehinmitola, E.; Adebimpe, A.; Shittu, T.; Solomon, B. Prospects of Biodiesel Feedstock as an Effective Ecofuel Source and Their Challenges. In *Advances in Eco-Fuels for a Sustainable Environment*; Woodhead Publishing: Sawston, UK, 2019; pp. 53–87.
10. Das, P.; Gundimeda, H. Is biofuel expansion in developing countries reasonable? A review of empirical evidence of food and land use impacts. *J. Clean. Prod.* **2022**, *372*, 133501. [[CrossRef](#)]
11. Knápek, J.; Králík, T.; Vávrová, K.; Valentová, M.; Horák, M.; Outrata, D. Policy implications of competition between conventional and energy crops. *Renew. Sustain. Energy Rev.* **2021**, *151*, 111618. [[CrossRef](#)]
12. Mairizal, A.Q.; Awad, S.; Priadi, C.R.; Hartono, D.M.; Moersidik, S.S.; Tazerout, M.; Andres, Y. Experimental study on the effects of feedstock on the properties of biodiesel using multiple linear regressions. *Renew. Energy* **2020**, *145*, 375–381. [[CrossRef](#)]
13. Mukhtar, A.; Saqib, S.; Lin, H.; Shah, M.U.H.; Ullah, S.; Younas, M.; Rezakazemi, M.; Ibrahim, M.; Mahmood, A.; Asif, S. Current status and challenges in the heterogeneous catalysis for biodiesel production. *Renew. Sustain. Energy Rev.* **2022**, *157*, 112012. [[CrossRef](#)]
14. Kamarulzaman, M.K.; Abdullah, A.; Mamat, R. Combustion, performances, and emissions characteristics of *Hermetia illucens* larvae oil in a direct injection compression ignition engine. *Energy Sources Part A Recovery Util. Environ. Eff.* **2019**, *41*, 1483–1496. [[CrossRef](#)]
15. Karthikeyan, S.; Prathima, A.; Periyasamy, M.; Mahendran, G. Assessment of the use of *Codium Decorticaefum* [Green seaweed] biodiesel and pyrolytic waste tires oil blends in CI engine. *Mater. Today Proc.* **2020**, *33*, 4224–4227. [[CrossRef](#)]
16. Branco-Vieira, M.; Mata, T.; Martins, A.; Freitas, M.; Caetano, N. Economic analysis of microalgae biodiesel production in a small-scale facility. *Energy Rep.* **2020**, *6*, 325–332. [[CrossRef](#)]
17. Tran, N.N.; Tišma, M.; Budžaki, S.; McMurchie, E.J.; Ngothai, Y.; Morales Gonzalez, O.M.; Hessel, V. Production of Biodiesel from Recycled Grease Trap Waste: A Review. *Ind. Eng. Chem. Res.* **2021**, *60*, 16547–16560. [[CrossRef](#)]
18. Konur, O. Waste Oil-Based Biodiesel Fuels: A Scientometric Review of the Research. In *Biodiesel Fuels Based on Edible and Nonedible Feedstocks, Wastes, and Algae*; CRC Press: Boca Raton, FL, USA, 2021; pp. 599–622.
19. Fróna, D.; Szenderák, J.; Harangi-Rákos, M. The challenge of feeding the world. *Sustainability* **2019**, *11*, 5816. [[CrossRef](#)]
20. Kolet, M.; Zerbib, D.; Nakonechny, F.; Nisnevitch, M. Production of Biodiesel from Brown Grease. *Catalysts* **2020**, *10*, 1189. [[CrossRef](#)]
21. Mizik, T.; Gyarmati, G. Economic and sustainability of biodiesel production—A systematic literature review. *Clean Technol.* **2021**, *3*, 19–36. [[CrossRef](#)]
22. Kamarulzaman, M.K.; Abdullah, A. Multi-objective optimization of diesel engine performances and exhaust emissions characteristics of *Hermetia illucens* larvae oil-diesel fuel blends using response surface methodology. *Energy Sources Part A Recovery Util. Environ. Eff.* **2020**, 1–14. [[CrossRef](#)]
23. Ali, S.S.; Al-Tohamy, R.; Mahmoud, Y.A.-G.; Kornaros, M.; Sun, S.; Sun, J. Recent advances in the life cycle assessment of biodiesel production linked to azo dye degradation using yeast symbionts of termite guts: A critical review. *Energy Rep.* **2022**, *8*, 7557–7581. [[CrossRef](#)]
24. Skowronek, P.; Wójcik, Ł.; Strachecka, A. Fat body—Multifunctional insect tissue. *Insects* **2021**, *12*, 547. [[CrossRef](#)]
25. Manzano-Agugliaro, F.; Sanchez-Muros, M.; Barroso, F.; Martínez-Sánchez, A.; Rojo, S.; Pérez-Bañón, C. Insects for biodiesel production. *Renew. Sustain. Energy Rev.* **2012**, *16*, 3744–3753. [[CrossRef](#)]
26. Li, Q.; Zheng, L.; Cai, H.; Garza, E.; Yu, Z.; Zhou, S. From organic waste to biodiesel: Black soldier fly, *Hermetia illucens*, makes it feasible. *Fuel* **2011**, *90*, 1545–1548. [[CrossRef](#)]
27. Surendra, K.; Olivier, R.; Tomberlin, J.K.; Jha, R.; Khanal, S.K. Bioconversion of organic wastes into biodiesel and animal feed via insect farming. *Renew. Energy* **2016**, *98*, 197–202. [[CrossRef](#)]
28. Li, W.; Li, Q.; Zheng, L.; Wang, Y.; Zhang, J.; Yu, Z.; Zhang, Y. Potential biodiesel and biogas production from corncob by anaerobic fermentation and black soldier fly. *Bioresour. Technol.* **2015**, *194*, 276–282. [[CrossRef](#)]
29. Li, Q.; Zheng, L.; Qiu, N.; Cai, H.; Tomberlin, J.K.; Yu, Z. Bioconversion of dairy manure by black soldier fly (Diptera: *Stratiomyidae*) for biodiesel and sugar production. *Waste Manag.* **2011**, *31*, 1316–1320. [[CrossRef](#)]
30. Furman, D.P.; Young, R.D.; Catts, P.E. *Hermetia illucens* (Linnaeus) as a factor in the natural control of *Musca domestica* Linnaeus. *J. Econ. Entomol.* **1959**, *52*, 917–921. [[CrossRef](#)]
31. Wang, C.; Qian, L.; Wang, W.; Wang, T.; Deng, Z.; Yang, F.; Xiong, J.; Feng, W. Exploring the potential of lipids from black soldier fly: New paradigm for biodiesel production (I). *Renew. Energy* **2017**, *111*, 749–756. [[CrossRef](#)]

32. Tomberlin, J.K.; Sheppard, D.C. Factors influencing mating and oviposition of black soldier flies (Diptera: *Stratiomyidae*) in a colony. *J. Entomol. Sci.* **2002**, *37*, 345–352. [[CrossRef](#)]
33. Myers, H.M.; Tomberlin, J.K.; Lambert, B.D.; Kattes, D. Development of black soldier fly (Diptera: *Stratiomyidae*) larvae fed dairy manure. *Environ. Entomol.* **2014**, *37*, 11–15. [[CrossRef](#)]
34. Parra Paz, A.S.; Carrejo, N.S.; Gómez Rodríguez, C.H. Effects of larval density and feeding rates on the bioconversion of vegetable waste using black soldier fly larvae *Hermetia illucens* (L.), (Diptera: *Stratiomyidae*). *Waste Biomass Valorization* **2015**, *6*, 1059–1065. [[CrossRef](#)]
35. Sealey, W.M.; Gaylord, T.G.; Barrows, F.T.; Tomberlin, J.K.; McGuire, M.A.; Ross, C.; St-Hilaire, S. Sensory analysis of rainbow trout, *Oncorhynchus mykiss*, fed enriched black soldier fly prepupae, *Hermetia illucens*. *J. World Aquac. Soc.* **2011**, *42*, 34–45. [[CrossRef](#)]
36. Kamarulzaman, M.K.; Hafiz, M.; Abdullah, A.; Chen, A.F.; Awad, O.I. Combustion, performances and emissions characteristics of black soldier fly larvae oil and diesel blends in compression ignition engine. *Renew. Energy* **2019**, *142*, 569–580. [[CrossRef](#)]
37. Zheng, L.; Li, Q.; Zhang, J.; Yu, Z. Double the biodiesel yield: Rearing black soldier fly larvae, *Hermetia illucens*, on solid residual fraction of restaurant waste after grease extraction for biodiesel production. *Renew. Energy* **2012**, *41*, 75–79. [[CrossRef](#)]
38. John, C.B.; Raja, S.A.; Deepanraj, B.; Ong, H. Palm stearin biodiesel: Preparation, characterization using spectrometric techniques and the assessment of fuel properties. *Biomass Convers. Biorefinery* **2022**, *12*, 1679–1693. [[CrossRef](#)]
39. Liwarska-Bizukojc, E.; Ledakowicz, S. Stoichiometry of the aerobic biodegradation of the organic fraction of municipal solid waste (MSW). *Biodegradation* **2003**, *14*, 51–56. [[CrossRef](#)]
40. Dogan, B.; Cakmak, A.; Yesilyurt, M.K.; Erol, D. Investigation on 1-heptanol as an oxygenated additive with diesel fuel for compression-ignition engine applications: An approach in terms of energy, exergy, exergoeconomic, enviroeconomic, and sustainability analyses. *Fuel* **2020**, *275*, 117973. [[CrossRef](#)]
41. Misra, N.N.; Rai, D.K.; Hossain, M. Chapter 10—Analytical Techniques for Bioactives from Seaweed. In *Seaweed Sustainability*; Tiwari, B.K., Troy, D.J., Eds.; Academic Press: San Diego, CA, USA, 2015; pp. 271–287.
42. Bacha, J.; Freel, J.; Gibbs, A.; Gibbs, L.; Hemighaus, G. *Diesel Fuels Technical Review*; Chevron Production Company: San Ramon, CA, USA, 2007.
43. Pulkrabek, W.W. *Engineering Fundamentals of the Internal Combustion Engine*; Pearson Prentice Hall: Hoboken, NJ, USA, 2004.
44. Ganesan, V. *Internal Combustion Engines*; McGraw-Hill: New York, NY, USA, 1994.
45. Ganesan, V. *Internal Combustion Engines*, 3rd ed.; McGraw-Hill Education (India) Pvt Limited: Karnataka, India, 2008.
46. Atabani, A.E.; Silitonga, A.S.; Badruddin, I.A.; Mahlia, T.; Masjuki, H.; Mekhilef, S. A comprehensive review on biodiesel as an alternative energy resource and its characteristics. *Renew. Sustain. Energy Rev.* **2012**, *16*, 2070–2093. [[CrossRef](#)]
47. Altıparmak, D.; Keskin, A.; Koca, A.; Gürü, M. Alternative fuel properties of tall oil fatty acid methyl ester–diesel fuel blends. *Bioresour. Technol.* **2007**, *98*, 241–246. [[CrossRef](#)]
48. Pramanik, K. Properties and use of jatropha curcas oil and diesel fuel blends in compression ignition engine. *Renew. Energy* **2003**, *28*, 239–248. [[CrossRef](#)]
49. Kwanchareon, P.; Luengnaruemitchai, A.; Jai-In, S. Solubility of a diesel–biodiesel–ethanol blend, its fuel properties, and its emission characteristics from diesel engine. *Fuel* **2007**, *86*, 1053–1061. [[CrossRef](#)]
50. Mofijur, M.; Masjuki, H.; Kalam, M.; Atabani, A.; Arbab, M.; Cheng, S.; Gouk, S. Properties and use of *Moringa oleifera* biodiesel and diesel fuel blends in a multi-cylinder diesel engine. *Energy Convers. Manag.* **2014**, *82*, 169–176. [[CrossRef](#)]
51. Torres-Jimenez, E.; Jerman, M.S.; Gregorc, A.; Liseic, I.; Dorado, M.P.; Kegl, B. Physical and chemical properties of ethanol–diesel fuel blends. *Fuel* **2011**, *90*, 795–802. [[CrossRef](#)]
52. Kegl, B. Experimental investigation of optimal timing of the diesel engine injection pump using biodiesel fuel. *Energy Fuels* **2006**, *20*, 1460–1470. [[CrossRef](#)]
53. Raheman, H.; Phadatare, A.G. Diesel engine emissions and performance from blends of karanja methyl ester and diesel. *Biomass Bioenergy* **2004**, *27*, 393–397. [[CrossRef](#)]
54. Demirbas, A. Relationships derived from physical properties of vegetable oil and biodiesel fuels. *Fuel* **2008**, *87*, 1743–1748. [[CrossRef](#)]
55. Atmanli, A. Effects of a cetane improver on fuel properties and engine characteristics of a diesel engine fueled with the blends of diesel, hazelnut oil and higher carbon alcohol. *Fuel* **2016**, *172*, 209–217. [[CrossRef](#)]
56. Fayyazbakhsh, A.; Pirouzfard, V. Investigating the influence of additives-fuel on diesel engine performance and emissions: Analytical modeling and experimental validation. *Fuel* **2016**, *171*, 167–177. [[CrossRef](#)]
57. Jose, T.K.; Anand, K. Effects of biodiesel composition on its long term storage stability. *Fuel* **2016**, *177*, 190–196. [[CrossRef](#)]
58. Mosarof, M.; Kalam, M.; Masjuki, H.; Ashraf, A.; Rashed, M.; Imdadul, H.; Monirul, I. Implementation of palm biodiesel based on economic aspects, performance, emission, and wear characteristics. *Energy Convers. Manag.* **2015**, *105*, 617–629. [[CrossRef](#)]
59. Bhuiya, M.; Rasul, M.; Khan, M.; Ashwath, N.; Azad, A.; Hazrat, M. Prospects of 2nd generation biodiesel as a sustainable fuel—Part 2: Properties, performance and emission characteristics. *Renew. Sustain. Energy Rev.* **2016**, *55*, 1129–1146. [[CrossRef](#)]
60. Alptekin, E.; Canakci, M. Characterization of the key fuel properties of methyl ester–diesel fuel blends. *Fuel* **2009**, *88*, 75–80. [[CrossRef](#)]
61. Kinast, J.A. *Production of Biodiesels from Multiple Feedstocks and Properties of Biodiesels and Biodiesel/Diesel Blends: Final Report*; Report 1 in a Series of 6; National Renewable Energy Lab.: Golden, CO, USA, 2003.